Notes

A Unified Picture of Static and Dynamic Length Scales in Polymer Solutions

Takashi Uematsu,* Christer Svanberg, and Per Jacobsson

Department of Applied Physics, Chalmers University of Technology, SE-412 96 Göteborg, Sweden

Received March 7, 2005

Revised Manuscript Received April 19, 2005

In nondilute polymer solutions, the chains are highly congested with other chains. The various properties of the solutions thus become strongly dependent on polymer concentration, in contrast to the behavior of better investigated dilute solutions.[1−4] In the 1970s, de Gennes introduced the blob model together with the reptation concept,[1] which were later used to predict the complicated concentration dependence of the different properties over a wide range of concentrations.[1−4] For example, the concentration dependence of the mesh size of polymer networks, the network conformation, and the gyration radius of the polymer were predicted. Similarly, the concentration dependence of dynamic properties, such as the polymer self-diffusion and collective diffusion, were also predicted. These static and dynamic properties are fundamental in, for example, adsorption, adhesion, swelling, and viscoelasticity, which in turn are of importance for basic understanding of biomacromolecular networks.[5] Despite the success of the blob model in the semidilute regime,[2,3] the general applicability has been questioned since the experimental observations on the dynamics in concentrated solutions were in poor agreement with the model.[4] Recent work on collective diffusion and polymer self-diffusion has implied that the disagreement is due to the conventional treatment of the local solvent viscosity, which neglects the concentration dependence.[6−8]

Here, in a thorough investigation of the static and dynamic properties of polystyrene solutions, we present the first incontrovertible support for the applicability of the blob model from semidilute to highly concentrated solutions by taking the local solvent viscosity into account. Polystyrene solutions have been chosen since they are archetypal in this context, thus providing a wealth of literature data.

According to the blob model,[1,2] an individual chain in a nondilute solution is visualized as a succession of blobs, of radius ξ, in which the chain experiences no effective interactions with other chains. Thus, the segmental conformation of the chain inside the blob (denoted later as "the partial chain") is identical to that in a dilute solution (see Figure 1).

* To whom correspondence should be addressed: Tel +46-31-772 3352; Fax +46-31-772 2090; e-mail uematsu@fy.chalmers.se.

The model can be described by only two parameters: the number of monomers per blob, g, and ξ. The main results from the model[1−4,6] can be summarized as follows: With increasing polymer concentration, the parameters g and thereby ξ decrease due to decreasing interchain contact distance. When ξ decreases, different regimes with different concentration dependence of g and ξ are discerned. If the polymer is dissolved in a good solvent at sufficiently low concentrations, the partial chain is swollen ($\xi \sim g^{0.6}$). On the basis of scaling arguments,[1] it is found that $g \sim \phi^{-1.25}$, where ϕ is the polymer volume fraction, resulting in $\xi \sim \phi^{-0.75}$ in this semidilute regime (I) (see Figure 1). With increasing concentration, the scaling approach breaks down when the blob becomes smaller than the so-called thermal blob,[3,4,9] of diameter ξ_T, in which segmental stiffness prevents the chain from swelling. Consequently, above the corresponding polymer concentration, the swollen partial chain becomes ideal ($\xi \sim g^{0.5}$), then when ξ approaches the persistence length[9] (L_p), the partial chain becomes "flexible-rod-like"[6] ($\xi \sim g^1$), and finally when ξ approaches the bond length[9] (L_b), it becomes "rigid-rod-like"[6] ($\xi \sim L_b$). The concentration dependence of g experiences another crossover as the number of interchain contacts per blob increases with increasing concentration. According to mean-field arguments,[4,6] four power law regimes besides regime I are predicted: a marginal solvent regime (II), a Θ solvent regime (III), a flexible-rod regime (IV), and a rigid-rod regime (V). Figure 1 visualizes the complex theoretical picture from regime I to V, showing the resulting power law behaviors of ξ and g in each regime.

Various experimental techniques can give information related to ξ and g. For example, static techniques (small-angle X-ray[10−12] and neutron[11−13] scattering) yield the static correlation length,[2] ξ_s. Dynamic techniques (photon correlation spectroscopy, PCS,[4,6,7,14] thermal diffusion forced Rayleigh scattering, TDFRS,[15,16] and classical gradient diffusion, CGD[17]) give the dynamic correlation length,[2] ξ_h. From the blob model,[2] both correlation lengths will be directly related to ξ; however, the origin of the two is different. While ξ_s reflects the screening length for the static excluded volume, ξ_h reflects the screening length for hydrodynamic interactions. Theoretically, we expect the relation $\xi > \xi_h > \xi_s$ at least in regime I.[18] If we consider neutral polymer solutions, the static property of g, g_s, can be obtained from the osmotic pressure.[19] Similarly, the hydrodynamic property, the number of monomers, g_h, inside a radius ξ_h can be obtained from the osmotic rigidity.[19] Since $g_s \approx g$, we expect the relation $g_s > g_h$ at least in regime I. Here, we have examined the properties related to ξ and g using literature data[4,10−17,20−22] on nondilute polymer solutions of atactic polystyrene in toluene (M_w = 96 400−280 000 g/mol, $M_w/M_n < 1.08$)[23] and also new data on ξ_h for atactic polystyrene (M_w = 301 600 g/mol, M_w/M_n = 1.04) in toluene, obtained from PCS.

10.1021/ma050478t CCC: $30.25
Published on Web 06/16/2005

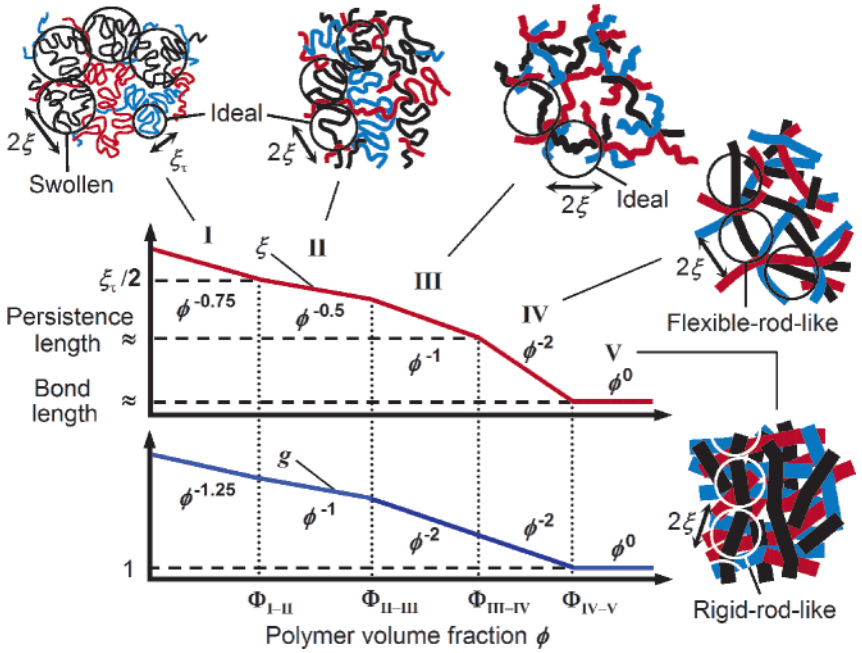

Figure 1. Schematic picture of polymer networks with increasing polymer volume fraction, ϕ, and a double-logarithmic schematic representation of the ϕ dependence of the blob radius, ξ, and the number of monomers, g, per blob. Roman numerals I−V indicate a semidilute, a marginal solvent, a Θ solvent, a flexible-rod, and a rigid-rod regime, respectively. The thickness and color of the solid lines in the schematic picture represent the approximate scale of each network and a single chain, respectively. ξ_τ is the thermal blob size. Φ_{i-j} denotes ϕ at the crossover from regime i to regime j. Note that blobs from regime I to IV are located within the interchain contacts.

(For the details see Supporting Information.) The overall data cover the concentration range from regime I to IV[19,24] or V.

In Figure 2A, we show ξ_s as a function of ϕ and a least-squares fit to the ξ_s data with fixed theoretical power law exponents for ξ, while the crossover volume fractions are free parameters. We find that the model can describe all the data despite the fact that the data is collected from several studies. These results are also corroborated by independent static data (g_s); a least-squares fit using the theoretical power law exponents for g to the g_s data shown in Figure 2B reveals a II/III crossover, consistent with the ξ_s crossover. (For details concerning the fitting procedure see Supporting Information.)

The dynamical correlation length (ξ_h) is derived via the Stokes−Einstein relation[25] using collective diffusion data obtained from the above-mentioned dynamic techniques.[2,4] Conventionally, the solvent viscosity term included in the Stokes−Einstein relation has been the neat solvent viscosity,[1,2,4] η_s (= 0.56 mPa s in the present system). The ξ_h derived using this approach gives little support to the theoretical model (see Figure 2A). Only one crossover, apparently from regime I to II, might be found for the high-M_w samples after a least-squares fit analysis. (For the details see Supporting Information.) A different approach[6,7] is to experimentally derive the so-called "effective local viscosity",[26] η_{eff}, from solvent self-diffusion data obtained via, for example, pulsed field gradient NMR. This technique can detect local solvent viscosity on the same time scale (i.e., millisecond time scale) as the dynamical methods (e.g., TDFRS, CGD) probe collective diffusion. It is to be noted that the time scale is of great importance since solvent dynamics measured on other time scales (e.g., picosecond time scale) yields rather different local solvent viscosity.[27] The accordingly obtained η_{eff} from the solvent self-diffusion data[21,22] in atactic polystyrene (M_w = 100 000−280 000 g/mol) solutions increases significantly at higher concentrations, in contrast to η_s, thereby following the predictions of a free-volume theory based model proposed by Vrentas and co-workers[28] for solvent dynamics in polymer solutions (see Figure 3A).

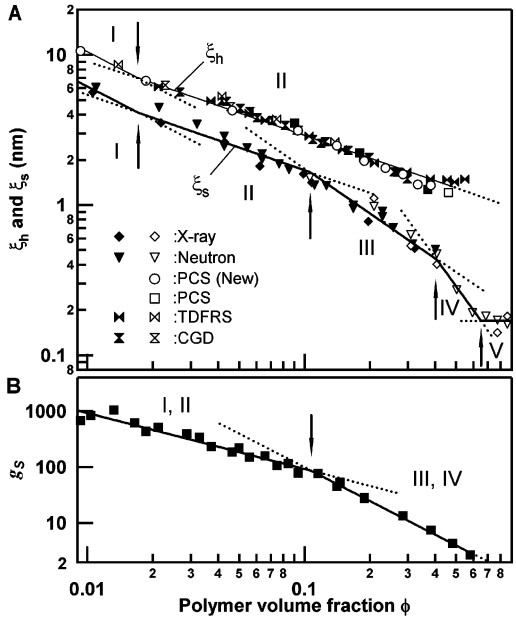

Figure 2. (A) Static correlation length, ξ_s, and the dynamic correlation length, ξ_h, derived using the neat solvent viscosity, vs polymer volume fraction, ϕ. The shapes of symbols indicate different techniques. (B) Number of monomers per blob, g_s, vs ϕ. The data presented in (A) and (B) are literature data and our new data (open circles) for polystyrene solutions in toluene at 25 °C. The solid and open symbols indicate data for 96 400 g/mol ≤ M_w < 190 000 g/mol and 190 000 g/mol ≤ M_w ≤ 301 600 g/mol, respectively. The solid lines represent least-squares fits using the theoretical power law exponents for ξ and g. The arrows and the dotted lines indicate crossovers between the different regimes numbered in roman numerals.

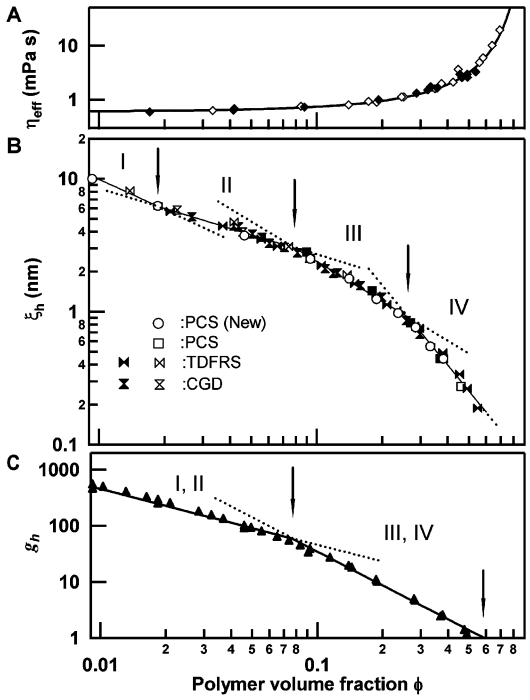

Figure 3. (A) Effective local viscosity, η_{eff}, vs polymer volume fraction, ϕ. The curve is from the free-volume theory fitted to the data. The free-volume parameters are consistent with the literature. (B) Dynamic correlation length, ξ_h, derived using the η_{eff} curve vs ϕ. The shapes of symbols are as Figure 2A. (C) Number of monomers, g_h, within $2\xi_h$ vs ϕ. In (A) to (C), the data are literature data and our new data (open circles) for polystyrene solutions in toluene at 25 °C. The solid and open symbols are as in Figure 2. In (B) and (C), the solid lines, the arrows, the dotted lines, and the roman numerals are as in Figure 2.

Figure 3B shows ξ_h vs ϕ when η_{eff} is taken into account. By applying a least-squares fit with the theoretical exponents for ξ, we find that the blob model now gives a good description of all the data covering the regimes from I to IV,[24] which has been indicated previously.[6] Furthermore, we performed complementary curve fit with also the four exponents as free parameters. Such a curve-fit procedure yields the exponents that are, within the errors, equal to their theoretical values. The observed crossover volume fractions except the I/II crossover volume fraction for ξ_h are slightly lower than those for ξ_s within the errors. The shift for the II/III crossover is theoretically expected due to their different physical origins.[29] The ξ_h data presented in Figure 3B are also corroborated by independent hydrodynamic g_h data; a least-squares fit using the theoretical power law exponents for g to the g_h data shown in Figure 3C reveals a II/III crossover in excellent agreement with the ξ_h crossover. A further quantitative agreement is found since the g_h value reaches unity at the concentration where ξ_h reaches the bond length (≈0.2 nm). (For details concerning the fitting procedure see Supporting Information.)

The blob model estimates that the crossover volume fractions for the I/II crossover and the II/III crossover are $\Phi_{I-II} = 162(1 - 2\chi)/(\pi C_\infty^3)$ and $\Phi_{II-III} \approx 1 - 2\chi$, respectively.[4] Here, χ is the Flory−Huggins interaction parameter, and C_∞ is the characteristic ratio. In our system,[30] $\chi \approx 0.43$ and $C_\infty = 9.85$, which yields $\Phi_{I-II} \approx 0.01$ and $\Phi_{II-III} \approx 0.1$. This result is consistent with the crossover values (see Supporting Information) found from the fit procedure for both static and dynamic data shown in Figures 2 and 3B,C.

The model predicts that the III/IV crossover occurs as a consequence of the partial chain becoming rodlike. On the basis of the results[31] on dilute solutions of atactic polystyrene in toluene, the rodlike transition will occur when ξ reaches ≈ 1.4 nm. In the present analysis, the III/IV crossover is observed when ξ_h (≈0.67ξ (see ref 18)) reaches ≈1 nm, in good agreement with the prediction.

To summarize, the theoretical picture of the length scales described by the combination of ξ and g is also valid for highly concentrated solutions when the local solvent viscosity is taken into account. Since the blob model is a general description of polymeric systems, the present findings will promote the fundamental understanding of various macromolecular systems, including natural polymers like DNA and actin filaments, over a wide range of polymer concentrations.

Acknowledgment. We thank A. Matic, R. Bergman, and D. Andersson for valuable discussions. This work was supported by the Swedish Foundation for Strategic Research.

Supporting Information Available: Details concerning the present PCS studies and the least-squares fit procedure. This material is available free of charge at the Internet at http://pubs.acs.org.

References and Notes

(1) de Gennes, P. G. *Scaling Concepts in Polymer Physics*; Cornell University Press: Ithaca, NY, 1979.
(2) Teraoka, I. *Polymer Solutions: An Introduction to Physical Properties*; Wiley-Interscience: New York, 2002.
(3) Rubinstein, M.; Colby, R. *Polymer Physics*; Oxford University Press: New York, 2003.
(4) Schaefer, D. W.; Han, C. C. In *Dynamic Light Scattering: Applications of Photon Correlation Spectroscopy*; Pecora, R., Ed.; Plenum: New York, 1985; pp 181−243.
(5) Boal, D. H. *Mechanics of the Cell*; Cambridge University Press: Cambridge, 2002.
(6) (a) Uematsu, T.; Svanberg, C.; Nydén, M.; Jacobsson, P. *Phys. Rev. E* **2003**, *68*, 051803. (b) Uematsu, T.; Svanberg, C.; Nydén, M.; Jacobsson, *AIP Conf. Proc.* **2004**, *708*, 205−208.
(7) Nicolai, T.; Brown, W. *Macromolecules* **1996**, *29*, 1698−1704.
(8) von Meerwall, E. D.; Amis, E. J.; Ferry, J. D. *Macromolecules* **1985**, *18*, 260−266.
(9) Norisuye, T.; Fujita, H. *Polym. J.* **1982**, *14*, 143−147. Typically, $\xi_\tau \approx 14$ nm and $L_p \approx 1$ nm for atactic polystyrene ($L_b \approx 0.2$ nm) in the good solvent benzene at 25 °C.; $\xi_\tau \approx 860$ nm and $L_p \approx 70$ nm for DNA ($L_b \approx 3.4$ nm; double-helix pitch) buffer solutions at 25 °C.
(10) Hamada, F.; Kinugasa, S.; Hayashi, H.; Nakajima, A. *Macromolecules* **1985**, *18*, 2290−2294.
(11) Kinugasa, S.; Hayashi, H.; Hamada, F.; Nakajima, A.; Kurita, K.; Nakajima, S.; Furusaka, M.; Ishikawa, Y. *Polym. Commun.* **1986**, *27*, 47−49.
(12) Brown, W.; Mortensen, K.; Floudas, G. *Macromolecules* **1992**, *25*, 6904−6908.
(13) King, J. S.; Boyer, W.; Wignall, G. D.; Ullman, R. *Macromolecules* **1985**, *18*, 709−718.
(14) Brown, W.; Johnsen, R. M.; Konak, C.; Dvoranek, L. *J. Chem. Phys.* **1991**, *95*, 8568−8577.
(15) Zhang, K. J.; Briggs, M. E.; Gammon, R. W.; Sengers, J. V.; Douglas, J. F. *J. Chem. Phys.* **1999**, *111*, 2270−2282.
(16) Rauch, J.; Köhler, W. *J. Chem. Phys.* **2003**, *119*, 11977−11988.
(17) Roots, J.; Nystöm, B. *Macromolecules* **1980**, *13*, 1595−1598.
(18) Muthukumar, M.; Edwards, S. F. *Polymer* **1982**, *23*, 345−348. A combination of path integral and field theoretic techniques predicts that $\xi_h/\xi_s = 32/9$ in regime I. Analogous to the case of dilute solutions,[2] we expect that $\xi/\xi_h \approx 1.5$ in regimes I, II, and III since ξ and ξ_h will correspond to the gyration radius and the hydrodynamic radius, respectively.
(19) The blob model predicts that, in analogy to the van't Hoff law, $\Pi \approx k_B T \times$ (the number of blobs in a unit volume),

where Π is the osmotic pressure, k_B is Boltzmann's constant, and T is the absolute temperature.[1−4] Thus, $g \approx \rho k_B T/\Pi \equiv g_s$, where ρ is the monomer number concentration. Furthermore, the model predicts that $D_c = E_0 g_h/(\rho\zeta)$, where D_c is the collective diffusion coefficient, E_0 is the osmotic rigidity, and ζ is the friction coefficient.[1,4] Thus, combining it with the Stokes−Einstein relation gives $g_h = \rho k_B T/E_0$. Note: the above two relations will collapse in regime V since the stiffness of the rigid-rod networks dominates the osmotic properties.

(20) (a) Higo, Y.; Ueno, N.; Noda, I. *Polym. J.* **1983**, *15*, 367−375. (b) Scholte, T. G. *Eur. Polym. J.* **1970**, *6*, 1063−1074. (c) T. G. Scholte, *J. Polym. Sci., Part A-2* **1970**, *8*, 841−868.

(21) (a) Pickup, S.; Blum, F. D. *Macromolecules* **1989**, *22*, 3961−3968. (b) Waggoner, R. A.; Blum, F. D.; MacElroy, J. M. D. *Macromolecules* **1993**, *26*, 6841−6848.

(22) Bezrukov, O. F.; Budtov, V. P.; Nikolayev, B. A.; Fokanov, V. P. *Polym. Sci. U.S.S.R.* **1971**, *13*, 988−996.

(23) The polystyrene used in some of the references (i.e., refs 12, 14, 21, and 22) was relatively polydisperse. However, the polydispersity does not significantly influence nondilute systems.[6a,7,21a]

(24) In this note, the ξ_h data are not included at concentrations where regime V is expected since we expect that the rigid-rod networks hinder the collective diffusive process of "*whole*" partial chains. As a consequence of the hindered process, an extra relaxation process arising from, for instance, the α-process is observed in this regime.[14,16]

(25) The Stokes−Einstein relation used for deriving ξ_h is $\xi_h = k_B T/(6\pi\eta D_c)$, where D_c is the collective diffusion coefficient, taking account of the solvent backflow, and η is the solvent viscosity.[1,2,4,6]

(26) The effective local viscosity[6,7] can be obtained via the Stokes−Einstein relation: $\eta_{eff} = k_B T/(6\pi D_{sol} R_{sh})$, where D_{sol} is the solvent self-diffusion coefficient and R_{sh} is the hydrodynamic radius of the solvent molecule (≈0.15 nm in the present system).

(27) Floudas, G.; Steffen, W.; Fischer, E. W.; Brown, W. *J. Chem. Phys.* **1993**, *99*, 695−703.

(28) Vrentas, J. S.; Duda, J. L. *J. Polym. Sci., Polym. Phys. Ed.* **1977**, *15*, 403−416.

(29) According to ref 18, the hydrodynamic properties (ξ_h and g_h) can exhibit a II/III crossover while static two-body interchain interactions still dominate at relatively low concentrations. On the other hand, from theoretical results (e.g., Muthukumar, M. *J. Chem. Phys.* **1986**, *85*, 4722−4728), the crossover for the static properties (ξ_s and g_s) can be expected only when static three-body interchain interactions become dominant at higher concentrations.

(30) Schuld, N.; Wolf, B. A. In *Polymer Handbook*, 4th ed.; Brandrup, J., Immergut, E. H., Grulke, E. A., Abe, A., Bloch, D. R., Eds.; Wiley-Interscience: New York, 1999; Chapter VII, p 247.

(31) Hayward, R. C.; Graessley, W. W. *Macromolecules* **1999**, *32*, 3502−3509.

MA050478T